Measuring and Reporting High Quality Factors of Inductors Using Vector Network Analyzers

William B. Kuhn, *Senior Member, IEEE*, and Adam P. Boutz, *Member, IEEE*

***Abstract*—Accurate measurement of high quality factors in inductors is a challenging task. While Q values in the range of 30 and below can be assessed using network analyzers with standard calibration techniques, reporting Q values of 50 or higher demands careful consideration of the type of calibrations used, the accuracy of the instrumentation and associated reference standards, and of the effects of the testing structures involved. This paper examines the accuracy of network analyzers operating in the VHF through S-band range with short-open-load calibrations, and shows that these common instruments can provide accurate Q measurements up to several hundred or more, but only if special care and methods are used.**

***Index Terms*—Accuracy, inductors, quality factor, resonant circuits.**

I. Introduction

FROM THE dawn of radio and electronics, inductors have played a crucial role in circuit design, yet high-quality inductors remain difficult to realize, especially as modern technologies attempt to reduce product size. Real-world inductors have significant series resistance and parallel capacitance that limit their lower and upper frequencies of operation, respectively. Series resistance, in particular, has a strong influence on the performance of circuits in which the inductor is used and is a problem at all frequencies. This parameter is typically quantified in terms of the inductor's quality factor Q, given as the ratio of the reactive part of the impedance Z to the resistive part as follows:

$$Q = \frac{\mathrm{Im}\{Z\}}{\mathrm{Re}\{Z\}}. \tag{1}$$

More fundamentally, Q is defined in terms of the peak energy stored divided by the energy dissipated per cycle

$$Q = 2\pi \frac{E_{\mathrm{peak}}}{E_{\mathrm{diss}}} \tag{2}$$

which gives the same result as (1), if and only if the inductor has no parasitic capacitance. If parasitic capacitance is present, then (1) goes to zero at the inductor's self-resonant frequency, leading to misleading (and unhelpful) data for resonant circuit designs [1]. Nevertheless, (1) is typically quoted, and we will use it in portions of this paper, with the understanding that it gives pessimistic results for circuit performance when operating close to self-resonance. For operating close to an inductor's self-resonant frequency or when using resonance techniques to measure Q, the fundamental definition and its related forms in terms of resonant-circuit bandwidth B versus center frequency f_0 should be used as follows:

$$B = \frac{f_0}{Q}. \tag{3}$$

Reported peak inductor quality factors have ranged from less than 10 in early RF integrated circuits (RFICs) [2], [3], to 30 or higher in some silicon-on-insulator processes [1]. Still higher values are possible if microelectromechanical (MEMs) techniques are employed [4] or if hybrid approaches are adopted where critical inductors are moved off-chip to printed circuit boards or low-temperature co-fired ceramic (LTCC) substrates. In such cases, Q's of up to 100 or higher are potentially obtainable and, indeed, have been reported [5].

Reporting Q values in the range of 50 or higher, however, requires more attention to the measurement techniques, equipment limitations, and quantification of error sources than most researchers have acknowledged. In this paper, we examine these accuracy issues in detail and present measurement techniques for assessing Q's of 50 or higher, with realistic precision. Emphasis is placed on adapting these techniques to use with vector network analyzer (VNA) equipment, since this is the instrument of choice for most practicing RF engineers. By quantifying the typical performance of VNAs in different regions of the Smith chart, we show that Q's from 50 to several hundred or more can be measured and reliably reported to two significant digits, without extraordinary equipment investments and setups.

II. Measurement Limitations of VNAs

Fig. 1 shows a typical one-port measurement of a high-Q inductor. At the marker frequency of 500 MHz, the measured impedance value is displayed as $2.121 + \mathrm{j}77.720$, implying a Q of $77.72/2.121 = 36.64$, based on (1). However, when reporting this value, the third and fourth significant digits are almost certainly irrelevant and even the second significant digit should be questioned, since network analyzers have significant limitations on accuracy of the underlying reflection coefficient (gamma) being measured. These limitations make the displayed impedance values subject to significant accuracy

Manuscript received July 15, 2009; revised January 15, 2010. First published March 11, 2010; current version published April 14, 2010. This work was supported in part under a contract by Honeywell Federal Manufacturing and Technologies' Kansas City Plant and Sandia National Laboratories.

W. B. Kuhn is with the Department of Electrical and Computer Engineering, Kansas State University, Manhattan, KS 66506 USA (e-mail: wkuhn@ksu.edu).

A. P. Boutz was with the Department of Electrical and Computer Engineering, Kansas State University, Manhattan, KS 66506 USA. He is now with Lockheed-Martin MS2, Eagan, MN 55121 USA (e-mail: adam.boutz@lmco.com).

Color versions of one or more of the figures in this paper are available online at http://ieeexplore.ieee.org.

Digital Object Identifier 10.1109/TMTT.2010.2042843

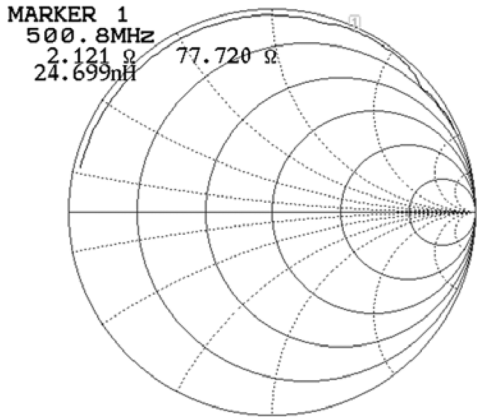

Fig. 1. Typical measurement of a high-Q inductor.

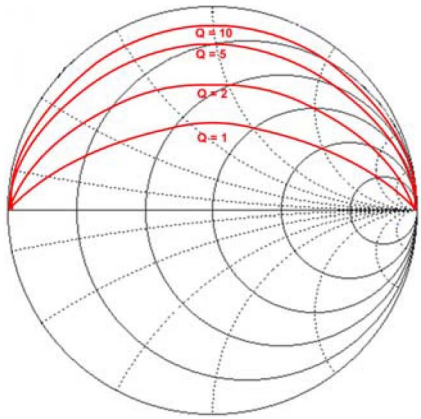

Fig. 2. Q contours plotted on a Smith chart.

limitations—especially when measuring impedances near the outer boundary of the Smith chart. For example, a typical VNA may be specified to have a gamma magnitude uncertainty on the order of 0.01 or 1% when measuring gamma magnitudes near one at UHF frequencies [6]. This uncertainty can increase to as high as 1.5% to 3% at higher frequencies, even after careful calibration with the latest instruments [7]. Such uncertainties can easily translate into errors of 50%–100% or more in Q.

A. Sensitivity of Q Accuracy to Gamma Errors

As with other quantities such as gain and noise figure, contours of Q can be plotted on a Smith chart. An example is shown in Fig. 2 for the definition of Q in (1). As Q increases, the contours move toward the outer boundary of the chart. In addition, all Q values converge at the $Z = 0$ and $Z = \infty$ points. This implies that Q values will be most accurate when the angle of gamma is close to 90 degrees. In particular, the most accurate region for measuring high Q, according to the definition of (1), is near the point $Z = +j\,Zo$.

Looking at this best-case point on the chart ($\angle\Gamma = 90°$), we can find the relationship between $|\Gamma|$ and Q from

$$Q = \frac{\mathrm{Im}\{Z\}}{\mathrm{Re}\{Z\}} = \frac{\mathrm{Im}\left[Zo\frac{1+j|\Gamma|}{1-j|\Gamma|}\right]}{\mathrm{Re}\left[Zo\frac{1+j|\Gamma|}{1-j|\Gamma|}\right]} = \frac{2|\Gamma|}{1-|\Gamma|^2}. \tag{4}$$

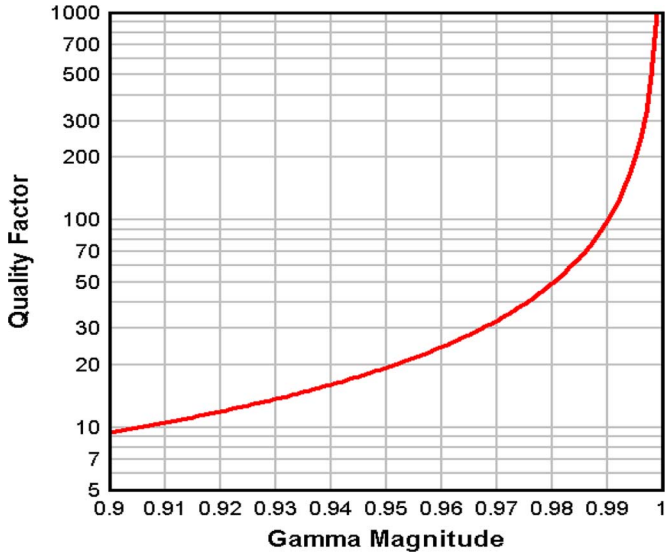

Fig. 3. Q versus Γ for best-case measurement ($\angle\Gamma = 90°$).

Fig. 3 plots Q versus gamma from (4) for the case of high-Q inductors with measured gamma values near the point $\Gamma = j$ for gamma magnitudes in the range of 0.9 to 0.999.

From this curve, it is clear that sensitivity to Γ errors increases dramatically at high Q and that an accuracy of significantly better than 1% is required to measure a Q of 100. For example, if the VNA gamma magnitude accuracy is ± 0.005 (which is approximately two times better than the stated accuracy of a typical instrument), a measured $|\Gamma|$ of 0.99 could imply a Q anywhere from 66 to 200.

Alternatively, we can use (4) to examine what accuracy on gamma is required to quote Q to two significant digits. Solving for $|\Gamma|$ in terms of Q yields

$$|\Gamma| = \sqrt{1 + \frac{1}{Q^2}} - \frac{1}{Q}. \tag{5}$$

Taking the series expansion of the first term and deleting higher order terms results in the approximate formula

$$|\Gamma| \approx 1 - \frac{1}{Q} \tag{6}$$

which is accurate to three significant digits for $\mathrm{Q} > 30$.

With (6), we can see that to quote a value of Q of 100 or higher to two significant digits requires an extraordinary accuracy on gamma. For example, to quote $Q = 110$ (i.e., to imply that Q lies between 105–115) requires knowing gamma to within the range of 0.9905–0.9909 or ± 0.0002. This is 50 times better than the stated accuracy. Indeed, for higher Q's or for inductors with values significantly away from the optimal point on the chart at $Z = +j50$, the accuracy requirement is even more stringent—and implausible.

B. Calibration Methods

The type of calibration and the calibration standards used can have a significant impact on the accuracy of measurements. For low-frequency analyzers such as the HP/Agilent 8753 series,

Fig. 4. Measurement of Line-1 after calibrating with HP85032 SOL standards shown.

TABLE I
GAMMA MAGNITUDES/PHASES (IN DEGREES) MEASURED ON MULTIPLE NETWORK ANALYZERS, AFTER USING PRECISION AND DEGRADED CALIBRATION STANDARDS (SEE TEXT AND FIG. 4)

Frequency	*Short*	*Open*	*Shorted Line-1*	*Shorted Line-2*
30 MHz	1.0004 / 179.6	1.0001 / -0.44	0.9990 / 176.5	0.9982 / 175.6
	1.0001 / 179.6	1.0004 / -0.44	0.9993 / 176.5	0.9980 / 175.6
	0.9999 / 179.6	0.9999 / -0.45	0.9988 / 176.5	0.9977 / 175.6
	1.0000 / 179.6	**1.0000 / -0.45**	**0.9987 / 176.5**	**0.9977 / 175.6**
	0.9997 / 179.6	**1.0000 / -0.45**	**0.9986 / 176.5**	**0.9974 / 175.6**
100 MHz	1.0003 / 178.7	0.9997 / -1.5	0.9982 / 168.4	0.9958 / 165.5
	1.0000 / 178.7	1.0006 / -1.5	0.9985 / 168.4	0.9960 / 165.5
	0.9996 / 178.7	1.0000 / -1.5	0.9978 / 168.4	0.9952 / 165.5
	0.9998 / 178.7	**1.0000 / -1.5**	**0.9967 / 168.4**	**0.9943 / 165.5**
	0.9996 / 178.7	**1.0000 / -1.5**	**0.9972 / 168.4**	**0.9943 / 165.5**
300 MHz	1.0003 / 176.2	0.9999 / -4.5	0.9965 / 145.4	0.9904 / 136.8
	1.0000 / 176.2	1.0003 / -4.5	0.9976 / 145.5	0.9914 / 136.7
	0.9993 / 176.1	1.0000 / -4.6	0.9962 / 145.4	0.9895 / 136.7
	0.9999 / 176.2	**1.0000 / -4.5**	**0.9918 / 145.6**	**0.9850 / 137.0**
	0.9993 / 176.1	**1.0000 / -4.6**	**0.9919 / 145.6**	**0.9845 / 137.0**
1 GHz	0.9996 / 167.4	1.0003 / -14.8	0.9942 / 67.6	0.9805 / 38.2
	0.9999 / 167.3	1.0003 / -14.8	0.9997 / 67.4	0.9847 / 37.6
	0.9993 / 167.0	1.0000 / -15.2	0.9943 / 67.6	0.9808 / 37.9
	0.9998 / 167.4	**0.9999 / -14.8**	**0.9975 / 68.9**	**0.9834 / 39.4**
	0.9984 / 167.0	**1.0000 / -15.2**	**0.9984 / 68.9**	**0.9839 / 39.0**
3 GHz	0.9994 / 142.0	1.0006 / -44.6	1.0004 / -150.0	0.9787 / 120.9
	0.9974 / 142.1	1.0002 / -44.8	0.9879 / -150.5	0.9768 / 121.1
	0.9974 / 141.2	1.0001 / -45.5	1.0004 / -150.3	0.9774 / 120.2
	0.9996 / 142.1	**1.0001 / -44.5**	**0.9623 / -150.0**	**0.9934 / 120.7**
	0.9974 / 141.2	**1.0000 / -45.5**	**0.9633 / -150.5**	**0.9924 / 120.2**

short-open-load-thru (SOLT) calibrations are the only type supported. Indeed, even for other analyzers, SOLT calibration is by far the most common method used [8]. For these reasons, we concentrate on this technique in the sections below.

For higher frequency use, analyzers with four-port samplers typically offer additional methods such as thru-reflect-line (TRL), line-reflect-match (LRM), and line-reflect-reflect-match (LRRM) [8]. In addition, advanced techniques that move calibration standards on-chip can increase accuracy [8], [9]. A thorough discussion of these methods is beyond the scope of this paper. However, specifications of modern analyzers [7], research on calibration accuracy [10], and the strong sensitivity of Q to gamma (Fig. 3) suggest that, even with these approaches, reporting Q's in the range of 50 or higher demands a careful assessment of error sources and resulting Q uncertainty.

C. Typical Versus Stated Accuracy

The typical accuracy of instruments may be better than the guaranteed specifications given by a manufacturer. Indeed, assuming one has correctly entered calibration-parasitic data into a VNA and the calibration standards used are of high quality, then remeasurement of the standards after calibration should yield very precise results near the short, open, and load (SOL) standards typically used for lower frequency VNAs. At other locations on the Smith chart, the errors can be expected to grow.

For the assessments below, exploration of this issue consisted of presenting the analyzer with impedances that are typical of inductors with high Q. This was achieved by measuring high-quality shorted transmission lines. One of these lines (Line-1), shown in Fig. 4, was created from a male-N to male-N adapter with a female short placed at the end. The other (Line-2) consisted of an N-to-SMA adapter, a male–male SMA barrel, and a female SMA short. Line-2 was somewhat longer than Line-1 to provide larger inductive impedances at a given frequency and has a lower effective Q due to smaller diameters and higher adapter losses.

The results are shown in Table I. The first three entries in each cell of the table are for two different HP8753C instruments, each with HP85046A test-sets, and one HP8753E with integrated test-set, respectively. Each of the analyzers was stabilized for two hours and then aligned with an HP85032 calibration kit, with filtering and averaging enabled. The last two entries of each cell are for one of the HP8753C units and for the HP8753E, both using a degraded load standard during calibration (see Section II-D below).

At 1 GHz and below, the worst-case error in gamma magnitude is 0.0007 (0.07%) when remeasuring the short and open reference impedances after precision calibration. This high accuracy relative to the guaranteed performance of around 1% at 1 GHz is expected, since the impedances measured are the same as those used for the calibration. Phase variations relative to the nominal phases that result from the standard's parasitics are better than 0.2 degrees up to 1 GHz and are ignored since they are not strong factors in assessing Q. At 3 GHz, the worst-case error magnitude increases to 0.0026, which is also approximately one order of magnitude better than guaranteed performance specifications.

For the region of the chart that represents high-Q inductances (assessed in the Line-1 and Line-2 columns), the results are more difficult to interpret, but the uncertainty suggested by

the variability between instruments is clearly higher. Even for the case of a single instrument, the errors can be seen to be higher. For example, for the precision calibration cases (first three entries of each cell), the Shorted Line-1 column shows the magnitude of the reflection coefficient is monotonically decreasing with frequency up to 300 MHz for the HP8753C units and through 1 GHz for the HP8753E. This is in keeping with the expected increasing losses with frequency for a transmission line. However, the jump from 0.9976 at 300 MHz to 0.9997 at 1 GHz for the second HP8753C clearly indicates an error on the order of 0.002 (0.2%) or higher. For the HP8753E, as the frequency increases from 1 to 3 GHz, the implied error is of the order of 0.006 (0.6%) or higher due to the increase in gamma from 0.9943 to the clearly incorrect value of 1.0004.

Examining the variation between instruments suggests even higher uncertainties. For example, at 1 GHz, the Line-1 column shows a disagreement of more than 0.005 (>0.5%) within the inductive region at 1 GHz.

Thus, in summary, the calibration verification tests indicate that the actual uncertainty in measurements can be up to 0.5% in the region of the chart that represents inductances. At this level of error, (4) shows that an inductor with an actual Q of 100 may measure anywhere from 67 to 200, even with this best-case calibration.

D. Effects of Imperfect Load Standards and Cables

The results above represent a best-case example, since they are based on high-precision references (standards) provided in connectorized calibration kits (cal-kits). For measurements made on an inductor using interconnecting cables, probes, and an imperfect calibration substrate, the measurements will be degraded by additional error sources. Cable impedance mismatch and imperfect calibration substrate impedances in particular can be expected to lead to significant degradation in accuracy above the 0.2%–0.5% uncertainties found above.

To assess this issue, the precision load standard was replaced with a Pasternack SM4226 N-to-SMA adapter terminated in a Minicircuits STRM-50 SMA load during calibration of the instruments. The impedance of this load ranged from $49.9+j\,0.10\ \Omega$ at 30 MHz to $51.2+j\,0.51\,\Omega$ at 1 GHz, and $48.6-j\,1.47\,\Omega$ at 3 GHz. These impedances correspond to return losses of 57, 38, and 34 dB, respectively. Thus, they represent an imperfect but still high-quality measurement setup.

Following calibration using this degraded standard, measurements of the short and open standards and of the two lines were conducted and are recorded in the last two entries in each cell of Table I (the first done on an HP8753C and the second with the HP8753E). Studying this data, we conclude that errors in gamma magnitude increase dramatically with load-standard errors and can be as high as 2%-4% at 1–3 GHz, respectively.

As a graphic example of these effects on measured Q, Fig. 5 shows the precision and degraded calibration results from zero to 1 GHz. For the precision case using the cal-kit load standard, the displayed data indicates a Q of $74.8/0.46 = 160$ at 1 GHz. For the degraded load-standard case, the suggested Q is $72.9/0.11 = 660$. Clearly, the second result is far less accurate, as evidenced by the imperfect tracking of the Smith chart's outer circle boundary.

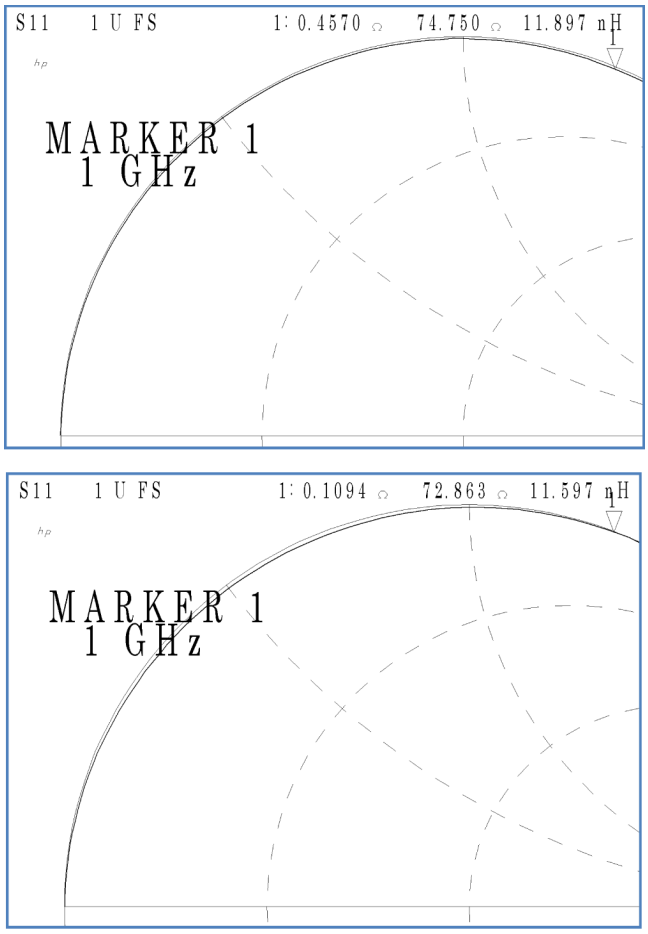

Fig. 5. Measurement of shorted line using precision *(top)* versus degraded *(bottom)* calibration load standards.

E. One-Port Versus Two-Port Measurements

While it has been shown that a multiport measurement with a network analyzer can be more accurate due to the extra terms in the error correction offered by extra standards [11], economy and mid-level analyzers do not offer the four-sampler capability needed for this enhancement. Moreover, measuring an inductor with a two-port setup requires collecting all four S-parameters and mathematically solving for Q. The errors in the three additional measurements may then compound the inductor Q uncertainty, and it seems unlikely that the final result will be significantly better than the case examined above. Determining if this is the case is beyond the scope of this paper. Instead, we pursue resonance-based techniques in the sections below and demonstrate how Q accuracy can be dramatically improved even with lower cost instrumentation.

III. Alternative Q Measurement Techniques

Creating resonant circuits to measure Q has been used for many decades [12]. For example, the HP 4342A RF Q meter manufactured by the Hewlett-Packard Company in the 1960s measured Q by resonating an inductor with a high-quality variable capacitor and measuring the voltage produced across the capacitor, as shown in Fig. 6 [13]. The instrument was capable of measuring Q's from 5 to 1000 at frequencies up to 70 MHz.

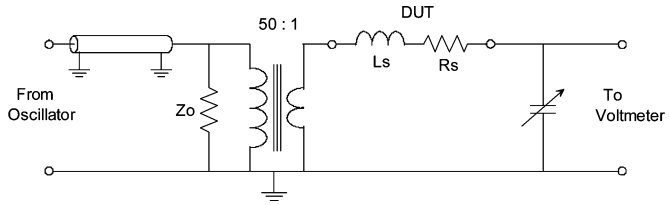

Fig. 6. Circuit used in HP4342A (after [13]).

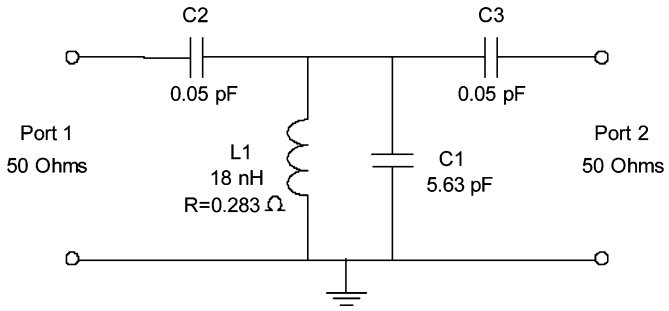

Fig. 7. Measuring the response of a parallel resonant circuit formed around the inductor.

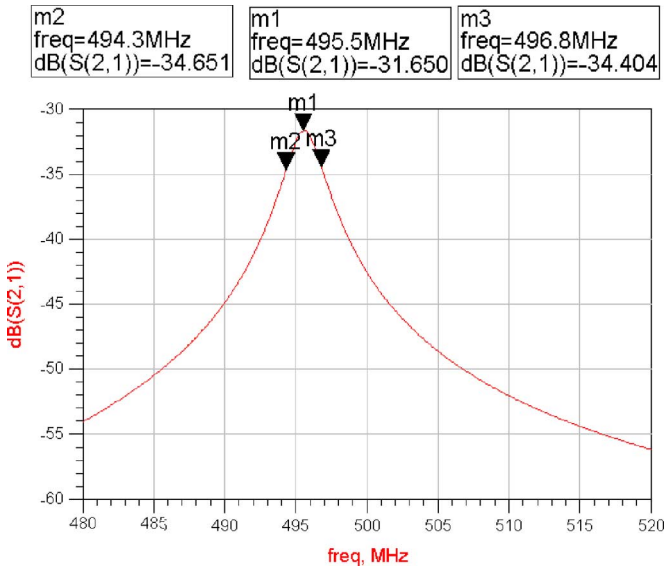

Fig. 8. Simulated S_{21} response of Fig. 7.

The technique relies on the fact that a series-resonant circuit develops a voltage across the capacitor equal to Q times the excitation voltage, so that by displaying the RF voltage across the capacitor with appropriate scaling, the Q is shown. The limiting factor here is the ability to generate a sufficiently low impedance source as frequencies are increased above the VHF range. Additionally, in common with all methods relying on resonance, it is critical that the series resistance around the *RLC* path be less than that of the inductor being measured (or that it is well-known and can be subtracted accurately). Thus, the measured Q will be bounded by the capacitor and interconnect resistances as well.

An additional technique that is widely used is to measure the bandwidth of a filtering response created by a resonant circuit. This technique has been used in the Boonton 34A resonant coaxial line to measure very low-loss capacitor dissipation factors [14]. The stated accuracy is better than 20% for capacitor Q's up to about 2000, under certain conditions. Although designed for capacitor measurement, the technique has been used by at least one surface-mount inductor manufacturer to provide precision Q measurements as well [15]. The technique employs a coaxial line as a resonating element, and ultimate performance will depend on providing a suitably low-loss transmission line and knowing its loss characteristics to a high accuracy. While this functions well for chip capacitors (and possibly chip inductors), it is difficult to apply for devices such as on-chip inductors or integrated passives in LTCC. However, the general concept remains valid and can be adapted to VNA setups. Hence, it is examined in Sections III-A and B.

A. Two-Port Resonant-Circuit Q Measurement

Q measurement techniques based on resonant circuits can be created in either series or parallel form [13], [16]–[18]. Both use the approach of exciting the resonant circuit with a signal generator and then measuring the bandwidth of the response to get Q from (3).

The parallel resonant circuit technique is shown in Fig. 7. Port 1 in this figure represents a swept source with a 50-Ω impedance, while port 2 represents a response measurement, also at 50 Ω. This could be a simple S_{21} magnitude measurement on a network analyzer.

When taking this approach, it is important to address unloaded versus loaded Q, since the measurement system's terminations will introduce losses into the overall circuit. This issue is addressed by C2 and C3. These capacitors must be a small fraction of the resonating capacitor C1, in order to loosely couple the source and load, thereby minimizing Q degradation in the tank. For this example, the core tank circuit L1, C1 is resonated at 500 MHz, and the tank circuit Q is 200. Hence, the effective parallel loss resistance of the tank is 11.3 kΩ. Clearly, C2 and C3 cannot be avoided, since the Q would be degraded from 200 to less than one by a net 25-Ω loading of the terminations.

Setting C2 and C3 to be approximately 1/100 of the tank circuit C solves this problem, while introducing an acceptable 30-dB attenuation in the signal path response from source to load. With the values shown, the series combination of C2 and the 50-Ω source termination present an equivalent *RC* parallel circuit load on the tank of 811 kΩ in shunt with 0.0503 pF. Hence, the tank's 11.3-KΩ parallel resistance at resonance is only degraded to 11.0 kΩ and an accurate Q can be found directly from the bandpass response measured, even without backing-out the losses from the terminations. The simulated response of this circuit is shown in Fig. 8, where a precise 2.5-MHz bandwidth is found. This is exactly the value expected for a Q of 200 at 500 MHz (note the slight shift if resonance from 500 MHz due to the capacitive loading of 2×0.05 pF).

In principle, larger capacitors could be used and the calculated loading of the terminations could be removed from the measured results through suitable calculations. However, the accuracy of this would depend on the exact values of C2 and C3 and any associated parasitics. A more important consideration is the possibility of feed-through from the source to the

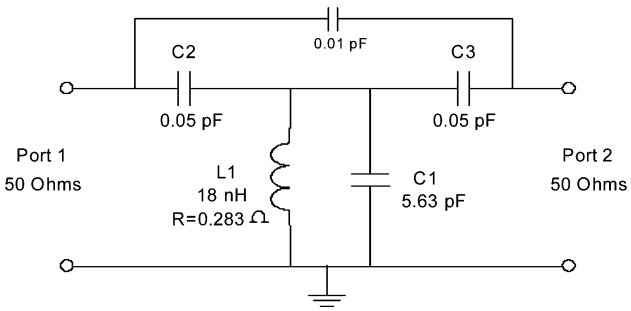

Fig. 9. Circuit of Fig. 7 with parasitic feed-through capacitance added.

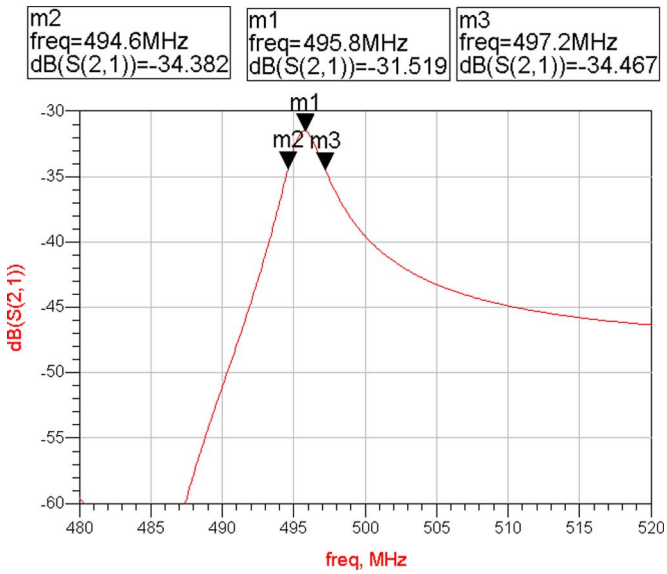

Fig. 10. Simulated S_{21} response of Fig. 9.

load due to fringing capacitances in an actual physical circuit. To investigate this source of error, Fig. 9 shows a model where the feed-through is 20% of the capacitance values of C2 and C3. The resulting response is shown in Fig. 10 and, while distorted, still displays the expected 2.5-MHz 3-dB bandwidth. Hence, this technique may still be viable for measuring Q's to 200 and above, if the feed-through capacitance can be suitably minimized.

The dual of the technique described above is illustrated in Fig. 11. Here, a resonating capacitor is added in series with the inductor being measured, and the source and load are coupled directly. This simpler arrangement can yield excellent results too, provided that the series tank circuit impedance at resonance (the series R of the inductor) is well below 50 Ω. Under this condition, the difference between loaded and unloaded Q will be negligible. Fortunately, for most high-Q inductors, this will be the case at the frequencies of interest.

The simulated response for the circuit of Fig. 11 is shown in Fig. 12. Note that the response here is on the order of −40 dB at resonance due to the low 0.283-Ω impedance presented at resonance. Moreover, the measured bandwidth is precisely 2.5 MHz as expected for a Q of 200 at 500 MHz, and no frequency shifting is created by the source and load. This type of response is easily measured with a modern network analyzer.

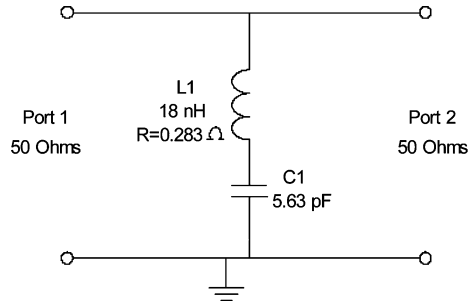

Fig. 11. Series resonant circuit stimulus-response measurement setup.

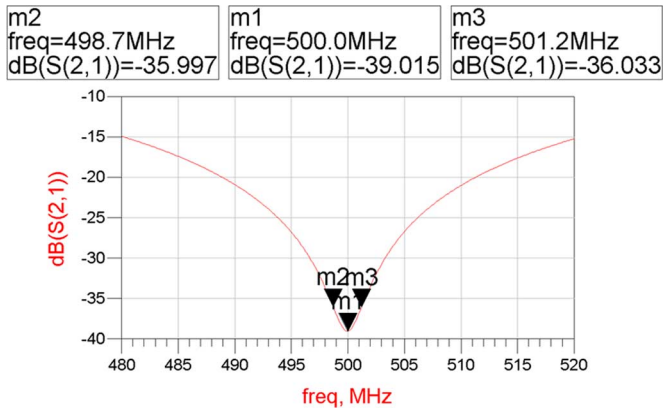

Fig. 12. Simulated S_{21} response of Fig. 11.

However, it is important to consider possible real-world circuit degradations for this technique as well. Feed-through capacitance is not an issue here, since the source and load connection points are the same, but contact resistance should be considered. Fortunately, this circuit shares many of the same features that a four-point probing technique offers to simple dc resistance measurements, and this is not a significant issue. However, one should consider the possibility of coupling in the measurement port probe tip area, especially if this is close to the inductor being measured. For accurate measurements based on 3-dB bandwidth or notch-depth assessments, this coupling must be small compared with the −40-dB S_{21} response.

B. One-Port Resonant-Circuit Q Measurement

A simpler and more direct approach, suggested by the results of Section II-C is to measure the resistance value of the series or parallel *RLC* circuit at the resonant frequency, using a VNA. For impedance measurement points on the Smith chart near the open and short circuits used during the calibration, high accuracy can be expected, as previously seen in columns 2 and 3 of Table I. This suggests that VNA impedance measurements taken near the very low resistance point of a series *RLC* circuit or the very high resistance point of a parallel *RLC* circuit may be sufficiently accurate, even when the calibration is imperfect. This is verified in the following section and used to illustrate that VNAs can be employed to make accurate measurements at Q values of several hundred or higher, if the inductor is resonated with a high-quality capacitor.

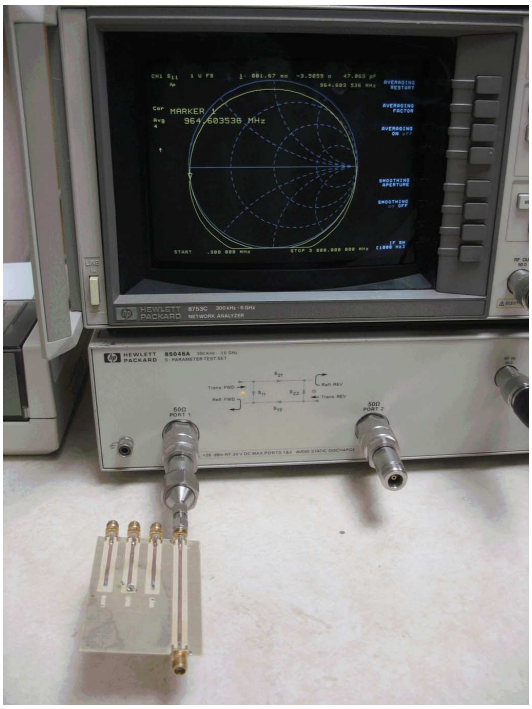

Fig. 13. Measurement of open-circuit line following calibration with imperfect microstrip SOL standards.

IV. Accuracy of Measuring Resonant Circuit R and Q With VNAs

If an inductor is resonated with a high-Q capacitor, the result will be either a very low resistance or very high resistance, depending on whether the capacitor is placed in series or parallel. In either case, to the extent that the measured value is near the calibration points, it can yield accurate Q measurements. This should be the case near the frequency of resonance, especially for calibration setups with small short/open parasitics, such as those found in probing environments.

To validate this statement, the performance of an HP8753C network analyzer was assessed near these points. A set of microstrip lines was created using low-loss 30-mil Rogers 4003C substrate material to form open, short, and load references. The lengths of the feeding lines were adjusted so that calibration parasitics of zero could be used for the short and open standards (close to what a probing environment allows at low gigahertz frequencies). However, while end-effect parasitics were minimized and line widths and SMA connector launches were implemented carefully, the realized impedance is not perfect. In addition, the load-standard consisted of a simple 0603 surface-mount resistor and therefore contained significant inductive parasitics. Hence, the load-standard's return loss was of the order of 25 dB. The effect on calibration can be seen in Fig. 13, where an unterminated line shows significant error (deviation from lying on the outer boundary) in the top and bottom halves of the chart.

Fortunately, the accuracy near the short and open impedance points is still high as previously discussed. To assess whether this accuracy is high enough to measure the resonant-circuit Q by measuring a resonant-circuit's resistance, several resistors were measured after calibration with this board. The results are shown in Fig. 14 and 15.

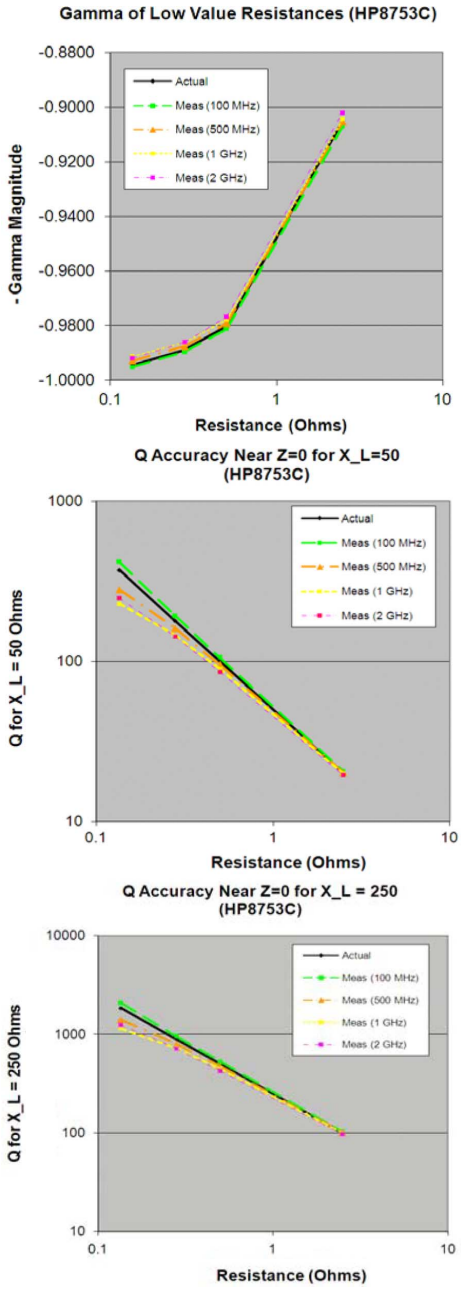

Fig. 14. Measurement of low resistances and calculated Q for inductor reactances of 50 and 250 Ω in a series *RLC* circuit.

Figs. 14 and 15 show the measured gamma values and the implied Q for example values of inductor and capacitor reactances (X) at the resonant frequency. To calculate the implied Q, the magnitude of the reflection coefficient was converted to a resistance value (R), and then the ratio X/R or R/X was plotted, as appropriate. In the conversion, the angle of gamma was ignored and only the magnitude was used, since an *RLC* resonant-circuit measurement would be taken at precisely 0 or 180 degrees. The actual measured angles were within a few degrees of the short and open locations and were therefore sufficiently close to the calibration points to yield good results. In a probing setup, the angle deviations would be even smaller.

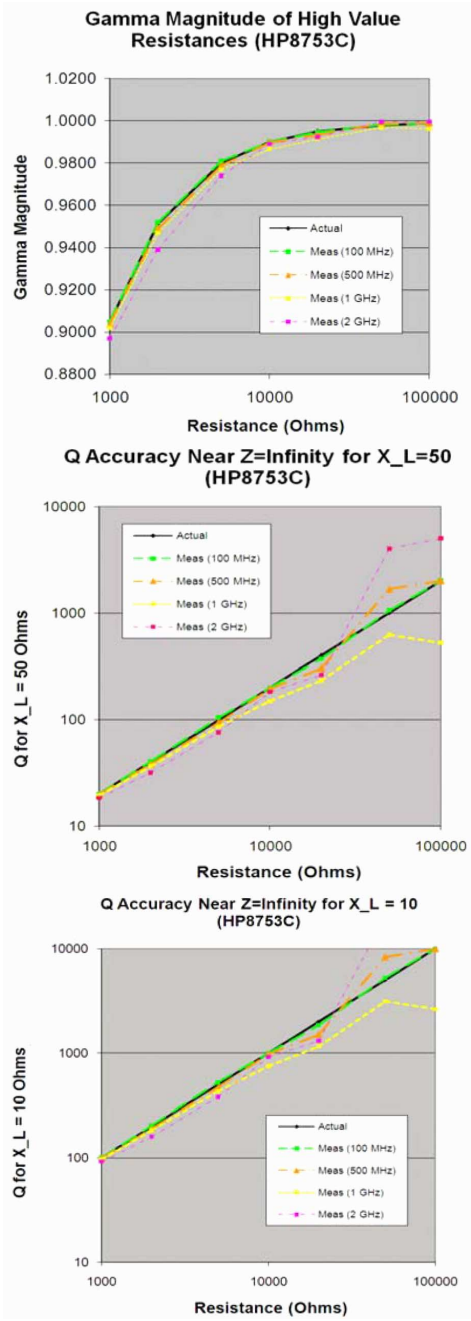

Fig. 15. Measurement of high resistances and calculated Q for inductor reactances of 50 and 10 Ω in a parallel *RLC* circuit.

The results shown indicate that Q's of up to 100 can be measured to two significant digits, and even values up to 1000 can be assessed with some degree of accuracy when the frequency and inductance yield X close to 50 Ω. For inductive reactances significantly higher or lower than 50 Ω, either the series or parallel modes will be preferred, respectively, and Q's of several thousand can potentially be measured with this simple method.

Finally, we note that these results can be considered to be conservative since the analyzer, interconnect lines, and standards used here are lower quality than those likely to be available in most laboratories, where high-performance cables, probing equipment, and calibration substrates would be used.

Fig. 16. Series *LC* circuit DUT.

TABLE II
MEASURED Q VALUES OF SURFACE-MOUNT 15-nH INDUCTOR USING MULTIPLE METHODS (SEE SECTION IV FOR ADDITIONAL NOTES)

Frequency (nominal)	Q from simple S11	Q from parallel R of LC circuit	Q from series R of LC circuit	Q using 2-port method of Fig. 11
500 MHz	22	59.0	59.5	60.0
1 GHz	14	105	85	90

V. EXAMPLE RESONANT-CIRCUIT Q MEASUREMENTS

To validate the proposed approaches, we measured the Q of a muRata LQW2BHN15NK13 15-nH high-Q (wire-wound) surface mount inductor at 500 MHz and 1 GHz, using multiple techniques. The measurements were taken after calibrating with the (imperfect) standards shown in Fig. 13. Following calibration, the inductor was attached at the end of the open line by adding a via to the backside, separated by 2 mm from the end of the line [for the 0805-size device-under-test (DUT)]. A simple S_{11} measurement was then taken and the Q was calculated. Next, an 0805 NPO ceramic capacitor (7 and 1.5 pF for the two frequencies) was added to form a parallel resonant circuit and the impedances at resonance were measured to find Q. Finally, the circuit was reconfigured to form a series resonator (see Fig. 16), and two methods were used to get Q. The series resistance at resonance was measured first and Q was found as X/R. Then, the series-resonant stimulus-response method of Fig. 11 was used, but with port 2 in the S_{21} measurement replaced with a 500-Ω termination consisting of probing with an HP54006 20-dB attenuating passive probe (following a through-calibration when probing at the end of a copy of the open-circuit line). The results are shown in Table II. For the resonance methods, actual frequencies varied from 456 to 469 MHz for the 500-MHz nominal case and 942 to 984 MHz for the 1-GHz case due to inductor/capacitor proximity and capacitive loading of the passive probe and have been accounted for in the reactances used to compute Q.

As expected from the imperfect calibration standards, the Q measured directly from S_{11} on the Smith chart with no capacitor is highly inaccurate. The low values shown are consistent with verification tests done following calibration, where a line with a reflection coefficient of close to one showed gamma values well inside the outer boundary in the upper half of the chart. However, even in the face of the significant calibration standard

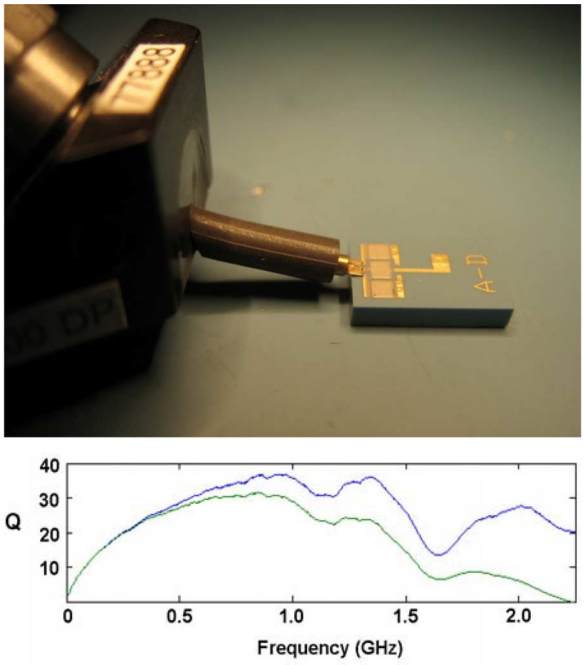

Fig. 17. Probing of LTCC embedded inductor and depression of Q due to radiation from dipole antenna formed by probe and DUT structure. Note the large pads used in the prototyping method of Fig. 7.

imperfections, the remaining techniques agree well with each other and with published data from the inductor manufacturer.

At 500 MHz, the measurements for all three techniques agree to two significant digits, so a third digit is shown in the chart to provide sufficient resolution for comparison. Using the combined measurements, the Q of the *LC* circuit can be confidently stated to be 59. At 1 GHz, the measurements show more variability, but the Q can be confidently stated to be around 95 ± 10. While such variation does not allow reporting Q to two significant digits, it is far better than the accuracy achievable with a direct S_{11} measurement, where even with a high-quality SOL calibration a 0.5% error in gamma can cause Q to vary from 67 to 200 (see Section II-D).

It should be emphasized that the high-precision test results reported in this section were achieved despite the degraded calibration described in Section IV, where the load standard was a simple 0603 resistor with a strong inductive component, and no parasitics were entered for the open and short standards. With a higher accuracy calibration, which is typical of a precision probing setup, up to two significant-digit precision may be possible even at 1 GHz and above.

VI. Coupling and Radiation Effects

Despite the good precision shown in Table II, the methods used here have the same hazards as those in any measurement of high-Q devices. In particular, two different mechanisms were found to degrade measurements during the course of this research.

First, as noted in Section III-A, the S_{21} measurements on systems such as those in Figs. 9 and 11 can be affected by coupling, either in the form of electric and/or magnetic fields—especially at higher frequencies. During the course of measuring S_{21} of the series *LC* circuit at 1 GHz, unrealistically sharp notch depths and bandwidths were noted. The sharp notch was traced to the presence of coupling from the microstrip line into the HP 54006 probe-tip structure. As confirmed by simulations, the induced voltage subtracted from and nulled the port-2 output, yielding an excessive notch depth.

Fortunately, the simpler short-circuit and open-circuit resistance measurements of the resonator do not experience this problem. However, even here, some degradation in Q was noted when the capacitor was located too close to the inductor, lowering its L value and introducing some eddy-current losses.

Finally, in measurements of inductors built in LTCC materials, radiation effects were noticed at certain frequencies. Fig. 17 shows an example case [19]. The two curves give the Q from a simple S_{11} measurement using the definitions of (1) for the lower curve and (2) for the upper curve [1], [19]. As seen in both curves, there is a significant dip in Q around 1.6 GHz for this device. The dip frequency was found to be independent of the DUT, and its origin was traced to the formation of a dipole-like antenna structure between the metal touched by the center probe lead and the ground structure formed by the probe body and connecting cable. Hence, hazards such as this must be recognized and avoided if possible in the design of the probing structures and setups to be used.

VII. Conclusion

VNAs are typically used to measure and report Q values of inductors. When Q is below approximately 30, these instruments can provide reasonable accuracy if careful calibration techniques and good-quality cables and standards are used. For measuring Q's of 50 and above, however, basic instrument limitations on gamma magnitude accuracy raise strong questions about reported measurement values. Gamma magnitude uncertainties of 1% will result in possible measurements ranging from 50 to infinity for an inductor with a true Q of 100. Assessment of measurement uncertainty indicates that published specifications may be conservative by a factor of about 2. However, as illustrated by Fig. 3, even with an uncertainty of 0.5%, reporting accurate Q values of 50 or higher with reasonable precision is unrealistic and other measurement approaches are required.

This paper has concentrated on assessing measurement accuracy for lower frequency analyzers which support SOLT-type calibrations. By confirming that such VNAs produce accurate measurements of impedances near the short, open, and load impedance values used in a one-port calibration, we have found that accurate measurements can be made and reported reliably with up to two significant digits for Q's of at least 50, and with confidence for up to 100 or more, but only if resonance techniques are used.

While we have focused on lower frequency analyzers and basic short-open-load calibrations, many of the accuracy considerations discussed here likely apply to instruments using more advanced calibrations at higher frequencies. Additional research is needed to assess the accuracy and precision to which inductor Q can be reported in those cases.

REFERENCES

[1] W. B. Kuhn, H. Xin, and M. Mojarradi, "Modeling spiral inductors in SOS processes," *IEEE Trans. Electron Devices*, vol. 51, no. 5, pp. 677–683, May 2004.

[2] N. M. Nguyen and R. G. Meyer, "Si IC-compatible inductors and *LC* passive filters," *IEEE J. Solid-State Circuits*, vol. 25, no. 4, pp. 1028–1031, Aug. 1990.

[3] J. N. Burghartz, M. Soyuer, and K. A. Jenkins, "Microwave inductors and capacitors in standard multilevel interconnect silicon technology," *IEEE Trans. Microw. Theory Tech.*, vol. 44, no. 1, pp. 100–104, Jan. 1996.

[4] D.-H. Weon, J.-H. Jeong, and S. Mohammadi, "High-Q micromachined three-dimensional integrated inductors for high-frequency applications," *J. Vac. Sci. Technol. B, Microelectron. Process. Phenom.*, vol. 25, no. 1, pp. 264–270, Jan./Feb. 2007.

[5] A. P. Boutz and W. B. Kuhn, "Measurement and potential performance of embedded LTCC inductors utilizing full tape thickness feature conductors," in *Proc. Ceramic Interconnect and Ceramic Microsystems Technologies*, 2009, pp. 259–264.

[6] *"HP 8753E RF Vector Network Analyzer, Technical Specifications"* 1998 [Online]. Available: http://www.home.agilent.com/upload/cmc_upload/All/LDC-5966-0054E-31842.pdf

[7] *"Agilent E5071C ENA Network Analyzer Data Sheet"* Jul. 30, 2009. [Online]. Available: http://cp.literature.agilent.com/litweb/pdf/5989-5479EN.pdf,

[8] "On-Wafer Vector Network Analyzer Calibration and Measurements," Cascade Microtech, Inc., Beaverton, OR, Application Note, 2002.

[9] A. Rumiantsev, S. L. Sweeney, and P. L. Corson, "Comparison of on-wafer multiline TRL and LRM+ calibrations for RF CMOS applications," in *Proc. 72nd ARFTG Microw. Meas. Symp.*, Dec. 9–12, 2008, pp. 132–136.

[10] R. F. Kaiser and D. F. Williams, "Sources of error in coplanar-waveguide TRL calibrations," in *Proc. 54th ARFTG Conf. Dig.*, Dec. 2000, vol. 36, pp. 1–6.

[11] J. A. Jargon, R. B. Marks, and D. K. Rytting, "Robust SOLT and alternative calibrations for four-sampler vector network analyzers," *IEEE Trans. Microw. Theory Tech.*, vol. 47, no. 10, pp. 2008–2013, Oct. 1999.

[12] *"4342A Q-meter Operating and Service Manual"* Mar. 1983 [Online]. Available: http://cp.literature.agilent.com/litweb/pdf/04342-90009.pdf

[13] W. Hayward, R. Cambell, and B. Larkin, "Experimental methods in RF design," *Amer. Radio Relay League*, p. 7.36, 2003.

[14] "Model 34A resonant coaxial line—A complete system for measuring the Q-factors of unleaded or leaded components at high frequencies," Boonton Electronics Corporation, Parsippany, NJ.

[15] B. N. Breen, C. Goldberger, and L. Talalaevsky, "The ACCU-L multi-layer induct4or for high frequency applications," *AVX Israel Ltd Tech. Inf. Bull.* [Online]. Available: http://avx.com/docs/techinfo/aculmlc.pdf

[16] D. Kajfez, S. Chebolu, M. R. Abdul-Gaffoor, and A. A. Kishk, "Uncertainty analysis of the transmission-type measurement of Q-factor," *IEEE Trans. Microw. Theory Tech.*, vol. 47, no. 3, pp. 367–371, Mar. 1999.

[17] D. Kajfez and E. Hwan, "Q-factor measurement with network analyzer," *IEEE Trans. Microw. Theory Tech.*, vol. MTT-32, no. 7, pp. 666–670, Jul. 1984.

[18] R. S. Kwok and J.-F. Liang, "Characterization of high-Q resonators for microwave-filter applications," *IEEE Trans. Microw. Theory Tech.*, vol. 47, no. 1, pp. 111–114, Jan. 1999.

[19] A. Boutz, "Inductors in LTCC utilizing full tape thickness features," M.S. thesis, Dept. Elect. and Comput. Eng., Kansas State Univ., Manhattan, 2009.

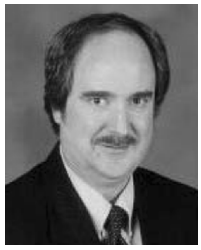

William B. Kuhn (SM'97) received the B.S. degree from the Virginia Polytechnic and State University, Blacksburg, in 1979, the M.S. degree from the Georgia Institute of Technology, Atlanta, in 1982, and the Ph.D. degree from the Virginia Polytechnic and State University in 1996, all in electrical engineering.

From 1979 to 1981, he was with the Ford Aerospace and Communications Corporation, Palo Alto, CA, designing satellite receiver equipment. From 1983 to 1992, he was with the Georgia Tech Research Institute, Atlanta, working on radar simulations and developing the XSPICE circuit simulator. In 1996, he joined Kansas State University, Manhattan, as an Assistant Professor, later becoming an Associate Professor in 2000 and Full Professor in 2006. He teaches courses in circuit design, communications theory, radio and microwave circuit/system design, and VLSI. His research is targeted at low-power radio electronics in CMOS, BiCMOS, GaAs, and SOI technologies and has ranged from characterization of spiral inductors to the design of radio receivers, transmitters, and power amplifiers.

Dr. Kuhn was the recipient of various awards ranging from the Bradley Fellowship in 1993 from the Virginia Polytechnic and State University to the Commerce Bank Award for Excellence in undergraduate teaching in 2008.

Adam P. Boutz (M'08) received the B.S. and M.S. degrees in electrical engineering from Kansas State University, Manhattan, in 2007 and 2009, respectively.

Since 2009, he has been with Lockheed Martin MS2, Eagan, MN, where he is involved in the development of RF-optical data links.